ISSN: 0369-8963

In order to represent how energy is dissipated in structures, various damping models have been developed to correlate analytical and experimental findings. One commonly used model is the Rayleigh viscous damping model, first introduced by Lord [1] and frequently used to describe energy dissipation in structural dynamics. This model describes the forces responsible for energy dissipation in a system as directly proportional to the velocity of the system's degrees of freedom (DOF). The equation of motion for a linear viscously damped system with N-DOF can be expressed as a set of coupled differential equations:

$$\mathrm{M}\ddot{\mathrm{q}}(t)+\mathrm{C}\dot{\mathrm{q}}(t)+\mathrm{K}\mathrm{q}(t)=\mathrm{f}(t) \tag{1}$$

$\mathrm{q}(t)\in\mathbb{R}^{N}$ represents the displacement vector, $\mathrm{f}(t)\in\mathbb{R}^{N}$ represents the force vector. For a linear damped discretized dynamic system, $\mathrm{M},\mathrm{C},\mathrm{K}\in\mathbb{R}^{N\times N}$ the mass, viscous damping, and stiffness matrices, respectively, the mass matrix is positive definite and symmetric, whereas the damping and stiffness matrices are semi-definite and symmetric. The damping matrix is assumed to be a linear combination of a system's mass and stiffness matrices in classical damping. This type of damping is referred to as Rayleigh damping. According to Caughey and O'Kelly [2], classical damping can be adequately described as a hypothesis that the damping matrix can be decoupled using undamped modes. Non-classical damping differs from classical damping; hence, the damping matrix does not depend only on a combination of the mass and stiffness matrices. Classical damping, in practice, ensures that energy is dissipated nearly equally throughout the system [3]. Non-classical systems may have highly damping components and related substructures with diverse characteristics. These damping representations may provide external damping to the systems in a manner different from the Rayleigh damping assumptions. When energy is dissipated in a structure in a non-uniform manner, complex mode forms emerge due to the non-classical distribution of damping. The damping non-classicality and the emergence of complex modes are discussed further in [4-6]. Thus the undamped modes of such systems cannot decouple the equation of motion. Common examples of non-classical damping in complex engineering applications are soil-structure interaction [7-9], composite and smart material structures [10-12], and the use of damping devices in structurally-controlled systems [13, 14]. Many experimental modal testing concluded that no physical system is rigorously classically damped; in most cases, the damping of linear systems is non-classical, according to Ma et al. [3].

Decoupling the non-classical linear damped systems must be accomplished by solving the quadratic eigenvalue problem (QEP) as shown in Eq. (2). Which can be obtained from checking the solution of the form $\mathrm{q}(t)=\psi\,\mathrm{e}^{\lambda t}$ in Eq. (1).

$$\left(\lambda_j^2\mathrm{M}+\lambda_j\mathrm{C}+\mathrm{K}\right)\psi_j=0,\qquad \forall j=1,2,\ldots,2N \tag{2}$$

https://doi.org/10.37896/pd92.4/9241

ISSN: 0369-8963

Since $\mathbf{M}, \mathbf{C}$ and $\mathbf{K}$ are all real matrices, assuming that the eigensolutions are distinct and there are no repeated roots. For a stable system, the eigensolutions appear in complex conjugation; the $\left(\lambda_j \in \mathbb{C}\right)$ is the complex eigenvalue and $\left(\psi_j \in \mathbb{C}^{2N\times 1}\right)$ is the corresponding complex eigenvector. Such eigenvalues problems are of great practical importance, which are discussed in detail by [15, 16]. The state-space method is frequently employed to obtain the exact solution to this quadratic eigenvalue problem. This method, also known as a linearization method, transforms the second-order eigenvalue problem into a first-order eigenvalue problem by doubling the size of the original system matrices; this procedure requires high calculation time. In addition, the physical significance of the solved system is lost due to the employment of sub-matrices of varying natures in this method [17].

Many studies suggest that it is more efficient to approximate non-classical eigensolutions than using the state-space method due to its high computation cost time. Several researchers have proposed sub-iteration methods to solve this eigenvalue problem [18-21]. Cha [22] presented a first-order approach that employs perturbation theory to compute the complex eigensolutions of linear viscous non-classical damping. Cortés and Elejabarrieta [23] have developed an approach to approximating complex eigensolutions in non-classical and non-viscously damped systems. Özgüven [24] provided a comprehensive review of the approaches used to decouple non-classically damped systems before 2002, contributing significantly to understanding this issue. Ma et al. [25] explained the differences in modal vectors between classical and non-classical damped systems. They introduced a phase-synchronization technique to transform non-classical analysis into the classical analysis. Adhikari [26] suggested an iterative method to find complex eigensolutions for non-classical viscous damped systems. This method only requires the eigensolutions of the undamped case, and the method combines the Galerkin minimization method and the Neumann expansion series to improve the approximation of the eigensolution iteratively. Lázaro [27] developed a mathematical expression to calculate the complex eigenvalues of non-classical viscously damped systems. This method uses undamped eigensolutions and perturbation techniques based on using Taylor series expansions. Lazaro incorporated the computed complex eigenvalues into a second-order expression proposed in [28] to determine the complex eigenvectors. Hračov and Náprstek [28] have proposed an approximation technique that employs a perturbation method to compute the complex eigensolutions of classically damped systems equipped with an additional passive damper.

In other research, Lázaro [29] suggests a fixed-point iteration method to determine the complex eigensolutions subject to non-classical and non-viscous damping systems. The assumptions underlying the new fixed-point iteration technique were initially based on the mathematical model and algorithm provided by [26, 30]. Sinha [31] introduced an iterative approach that employs the continuation method to compute the non-classical complex eigensolutions of repeated eigenvalue problems. Morzfeld et al. [32] introduced a technique for approximating the time history response of a non-classically damped system subjected to earthquake excitation. This method involves decoupling the quadratic eigenvalue problem of these systems. Denoël and Degée [33] suggested decoupling the non-classically damped system using an asymptotic expansion of the transfer functions.

 https://doi.org/10.37896/pd92.4/9241

ISSN: 0369-8963

It is essential to mention that the lightly non-classical damping method is critical in developing most of the approaches above. The lightly non-classical damping method is always used in deriving new and improved methods to decouple the non-classically linear damped systems. The lightly non-classical damping method is also known as the decoupling approximation method. It is based on the Rayleigh damping model and the forced orthogonality condition, which means ignoring non-diagonal terms of the modal damping matrix in approximating the complex eigenvalues. It is based on the Rayleigh damping model and the forced orthogonality condition, which means ignoring the non-diagonal terms of the modal damping matrix in approximating the complex eigenvalues. According to [34, 35], when dealing with highly non-classical damping systems, this approximation may result in modal coupling and fictional damping. This method is effective in obtaining complex eigensolutions for diagonally dominant systems. Extensive investigations into the accuracy of the lightly non-classical damping method have revealed that diagonality dominance is not a sufficient condition to rely on this method.

To fully decouple non-classically damped systems, it is necessary to replace the undamped modes with complex modes that account for the complexity of non-classical damping [36-38]. Therefore, Morzfeld et al. [39] proposed a study on the diagonal dominance of the damping matrix for non-classical viscous damped systems and established two indices for quantifying the degree of diagonality. Their study demonstrated that the choice of a diagonality index is insignificant in identifying error drifts due to the decoupling approximation *(i.e., using complex eigenvalues and real undamped eigenvectors to capture the system response)*. Koruk and Sanliturk [4] confirmed the results obtained by Morzfeld et al., thereby highlighting the importance of replication and verification in scientific research. To overcome this limitation, complex eigenvectors of diagonally dominant systems can be generated using simple mathematical formulations considering the imaginarity of the eigenvectors due to the off-diagonal terms of modal damping matrix, as demonstrated in [28, 30, 40].

This paper aims to explore alternative, cost-effective approaches to decoupling non-classical linear damped systems in structural dynamics. The objective is to replace the computationally expensive exact state-space approach with more efficient methods. The paper investigates two methods: the lightly non-classical damping method based on undamped eigenanalysis and the Adhikari first-order iterative algorithm, which employs the Neumann series and Galerkin error minimization techniques. The suitability of these methods for any non-classical linear damped system is determined using diagonality dominance indices. The paper proposes a new subspace algorithm that combines both techniques to enhance their effectiveness.

2 Mathematical formulations

2.1 State-space method

In order to evaluate the performance of alternative methods, the state-space method is considered the benchmark for computing the exact eigensolutions of the quadratic eigenvalue problem presented in Eq. (2). This method makes quadratic eigenvalue problems linear [41]. The equation of motion in Eq. (1) can be represented in the first-order form as expressed:

$$\mathrm{A}\dot{\mathrm{u}}(t)+\mathrm{B}\mathrm{u}(t)=\mathrm{g}(t) \tag{3}$$

$\mathrm{A},\mathrm{B}\in\mathbb{R}^{2N\times 2N}$ are defined as the state space system matrices, symmetric and real.

https://doi.org/10.37896/pd92.4/9241

ISSN: 0369-8963

$$\mathrm{A}=\begin{bmatrix}\mathrm{O} & \mathrm{M}\\ \mathrm{M} & \mathrm{C}\end{bmatrix},\quad \mathrm{B}=\begin{bmatrix}\text{-M} & \mathrm{O}\\ \mathrm{O} & \mathrm{K}\end{bmatrix},\quad \mathrm{u}(t)=\begin{bmatrix}\dot{\mathrm{q}}(t)\\ \mathrm{q}(t)\end{bmatrix},\quad \mathrm{g}(t)=\begin{Bmatrix}\mathrm{O}_{N\times 1}\\ \mathrm{f}(t)\end{Bmatrix} \tag{4}$$

$\mathrm{g}(t)\in\mathbb{R}^{2N\times 1}$ and $\mathrm{O}\in\mathbb{R}^{N\times N}$, respectively, represent the input vector and the null matrix. The eigensolutions can be determined by assuming that all the eigenvalues are distinct and solving the linearized eigenvalue problem by checking the solution of the form $\mathrm{u}(t)=\mathbb{Z}\mathrm{e}^{\lambda t}$ in Eq. (4), as follows:

$$\left(\lambda_j\mathrm{A}+\mathrm{B}\right)\mathrm{Z}_j=0,\qquad \mathrm{Z}_j=\begin{Bmatrix}\lambda_j\psi_j\\ \psi_j\end{Bmatrix} \tag{5}$$

$\lambda_j\in\mathbb{C}$ and $\mathrm{Z}_j\in\mathbb{C}^{2N\times 1}$, respectively, represent the complex eigenvalues and the complex eigenvectors. State-space method assumes a bi-orthogonality relationship exists between the system matrices $\mathrm{A}$and B. The computation complexity of the state-space method is $\mathrm{O}\left(2N\right)^3=\mathrm{O}\left(8N^3\right)$. For further discussion of state-space linearization approaches, refer to Walsh and Day [16].

2.2 Undamped eigenvalue problem

The undamped eigenvalue problem is fundamental for structural dynamics analysis, providing information about natural frequencies and vibration modes. Understanding undamped systems serves as a baseline for comparing the effects of damping. The equation of motion for free undamped vibration can be expressed as follows:

$$\mathrm{M}\ddot{\mathrm{q}}(t)+\mathrm{K}\mathrm{q}(t)=0 \tag{6}$$

The eigenvalue problem of the undamped system in Eq. (6) can be solved by assuming a solution of the form $\mathrm{q}(t)=\mathrm{q}\mathrm{e}^{\omega t}$, which yields *N*-degrees of freedom distinct eigenvalues $\left(\omega_j^2\in\mathbb{R}\right)$ and eigenvectors $\left(\mathrm{q}_j\in\mathbb{R}^{N\times 1}\right)$. Each mode of this distinct system can be expressed as follows:

$$\mathrm{K}\mathrm{q}_j=\omega_j^2\mathrm{M}\mathrm{q}_j \tag{7}$$

$\omega_j\in\mathbb{R}$ denotes the natural frequency of the undamped system. The eigenvector of the undamped system q_j can be normalized to have a generalized mass form as follow:

$$\mathrm{q}_k^T\mathrm{M}\mathrm{q}_j=\delta_{kj},\qquad \mathrm{q}_k^T\mathrm{K}\mathrm{q}_j=\omega_j^2\delta_{kj},\qquad \forall k,j=1,2,\ldots,N \tag{8}$$

δ_{kj} denotes the Kronecker delta function. The modal matrix represents the modal vectors assembled in a matrix form, and it can be expressed as:

$$\mathrm{Q}=\left[\mathrm{q}_1,\ \mathrm{q}_2,\ \ldots,\mathrm{q}_N\right]\in\mathbb{R}^{N\times N} \tag{9}$$

From Eq. (7-9), it is possible to conclude that the modal mass and stiffness matrices can be represented as:

$$\mathrm{M}'=\mathrm{Q}^T\mathrm{M}\mathrm{Q}=\mathrm{I}_N,\qquad \mathrm{K}'=\mathrm{Q}^T\mathrm{K}\mathrm{Q}\equiv\Omega^2=\mathrm{diag}\left(\left[\omega_1^2,\quad \omega_2^2\quad\cdots\quad \omega_N^2\right]\right) \tag{10}$$

https://doi.org/10.37896/pd92.4/9241

ISSN: 0369-8963

$\mathrm{I}_N \in \mathbb{R}^{N\times N}$ and $\Omega \in \mathbb{R}^{N\times N}$, respectively, are the identity matrix and the matrix of squared circular frequencies (undamped eigenvalues). The modal damping matrix can be expressed as:

$$\mathrm{C}' = \mathrm{Q}^T \mathrm{C} \mathrm{Q} \equiv \mathrm{C}'_d + \mathrm{C}'_o \tag{11}$$

$\mathrm{C}'_d, \mathrm{C}'_o \in \mathbb{R}^{N\times N}$ are respectively denote the diagonal and off-diagonal elements of the modal damping matrix. For further discussion on the modal damping matrix representation, refer to Gawronski and Sawicki [42].

2.3 Diagonality dominance indices

Many studies have attempted to characterize diagonal dominance for modal damping matrix to decide when decoupling approximation is appropriate. According to [39, 43], the modal damping matrix has a diagonal dominance only and only if the condition below holds for all the diagonal modal damping matrix elements, as follows:

$$|c_{jj}| \geq \sum_{\substack{k=1 \\ k\neq j}}^{N} |c_{jk}|, \qquad \forall k, j = 1, 2, \ldots, N \tag{12}$$

The non-classicality of the damping behavior of a system can be evaluated by examining the extent to which the diagonal elements of the modal damping matrix are dominant. When the modal damping matrix has highly dominant diagonal elements, the system behaves in a classically damped manner. On the other hand, when the non-diagonal terms dominate the modal damping matrix, the system exhibits non-classical damping behavior. Calculating the overall diagonality dominance index is necessary to determine if the lightly non-classical damping method is suitable for obtaining the complex eigensolutions of non-classically damped systems. The overall index allows identifying the system without seeking into every mode individually. Graham [44] showed that the modal damping matrix C' is diagonally dominating in a complete sense if and only if the spectral radius (highest absolute value of any eigenvalue of $\left(\left|\mathrm{C}'^{-1}_d\right|\left|\mathrm{C}'_0\right|\right)$ is less or equal to one). This overall diagonality dominance index can be expressed as:

$$\rho_1\left(\mathrm{C}'\right) = \max\left(\left|\mathrm{eig}\left(\mathrm{C}'^{-1}_d \mathrm{C}'_o\right)\right|\right) \leq 1 \tag{13}$$

If $\rho_1\left(\mathrm{C}'\right)$ is less or equal to one, the system is detected as diagonally dominant. Many publications have employed this index of diagonality dominance; see [33, 34, 45], since this index $\rho_1\left(\mathrm{C}'\right)$ needs the off-diagonal damping matrix's inverse. Due to the complexity of inverse calculation, another less complicated and more flexible overall index denoted by $\rho_2\left(\mathrm{C}'\right)$, and can be found in [34]. This diagonal dominance index can be calculated using the following expression:

$$\rho_2\left(\mathrm{C}'\right) = \frac{\sum_{j=1}^{N} \left|\mathrm{C}'_d\right|}{\sum_{j=1}^{N} \left|\mathrm{C}'_o\right|} \geq 1 \tag{14}$$

 https://doi.org/10.37896/pd92.4/9241

If $\rho_2(\mathrm{C}')$ is more or equal to one, the system is detected as diagonally dominant. A performance comparison between these two indices will be conducted in the results section.

2.4 Lightly non-classical damping method

The eigenvalue problem to the lightly non-classical damping method can be represented by reconstructing the equation of motion using the system's matrices in modal form by checking the solution $\mathrm{q}(t) = \mathrm{q}e^{\lambda t}$. The quadratic eigenvalue problem of the equation motion in Eq. (1) can be represented by modal system matrices as follows:

$$\left(\lambda_j^2 \mathrm{I}_N + \lambda_j \mathrm{C}' + \Omega^2\right)\mathrm{q}_j = 0, \qquad \forall j = 1, 2, \ldots, N \tag{15}$$

By supposing that the modal damping matrix is diagonal and neglecting its off-diagonal terms $\mathrm{C}'_o = 0$, the eigenvalues of the system λ_j, λ_j^* are calculated as follows:

$$\lambda_j, \lambda_j^* = -\frac{\mathrm{C}_{jj}}{2} \pm i\sqrt{\omega_j^2 - \left(\frac{\mathrm{C}_{jj}}{2}\right)^2} \tag{16}$$

$(\bullet)^*$ denotes the complex conjugation. For the lightly non-classical damping method, it is possible to compute the corresponding complex eigenvectors using Adhikari's first-order formula [30] as expressed in Eq. (17).

$$\psi_j = \mathrm{q}_j + \sum_{\substack{k=1 \\ k \neq j}}^{N} \frac{\lambda_j \mathrm{C}'_{kj}}{\omega_k^2 + \lambda_j^2 + \lambda_j \mathrm{C}'_{kk}} \mathrm{q}_k, \qquad \psi_j^* = \mathrm{conj}(\psi_j) \tag{17}$$

$\boldsymbol{\psi}_j$ denotes the corresponding complex eigenvector to the complex eigenvalue of the lightly non-classical damping method. This formula provides an additional decoupling of the undamped eigenvectors. This formula requires only the undamped eigensolutions and the modal damping matrix. This formula should be used; only if the system exhibits diagonality dominance. This process takes advantage of operation uniqueness while not relying on iteration. [27] first used a second-order expression of the formulation brought by Adhikari [30] to find the complex eigenvectors based on known complex eigenvalues. It is essential to note that the study presented by Lázaro [27] does not match the use of this formulation with the diagonality dominance. Moreover, the referred study uses a second-order formulation expression, while the current study uses a first-order one.

According to Ibrahimbegovic and Wilson [46], the computational complexity of the undamped eigenvalue problem used in the lightly non-classical damping method is $\mathrm{O}\left(N^3\right)$, makes this method less computationally expensive than the exact state-space method, which has a complexity of $\mathrm{O}\left(2N\right)^3 = \mathrm{O}\left(8N^3\right)$.

2.5 Adhikari's first-order iterative algorithm

Adhikari's first-order algorithm allows for the computation of a non-classically damped system's complex eigensolutions, starting from the undamped eigensolutions referring to [26]. This algorithm takes into consideration the fact that eigenvalues would be distinct and would come in complex conjugate pairs. This algorithm uses a mathematical framework that permits the iterative update of complex eigenvalues at each step. Which terminates by solving the eigenvalue problem in its original space as follows:

 https://doi.org/10.37896/pd92.4/9241

ISSN: 0369-8963

$$\left(\lambda_{j,Conv.}^2 \mathrm{M} + \lambda_{j,Conv.} \mathrm{C} + \mathrm{K}\right) \psi_{j,Conv.} = 0, \qquad \forall j = 1, 2, \ldots, N \tag{18}$$

$\lambda_{j,Conv.}$ and $\psi_{j,Conv.}$ are the convergent complex eigensolutions for the *j*-th mode. The lightly non-classical eigenvalues and the undamped eigenvectors serve as the initial conditions for the first step of the calculation. An updated complex eigenvalue $\lambda_j^{(r+1)}$ is calculated after each iteration. To determine this complex eigenvalue, the parameter $\eta_j\left(\lambda_j^{(r)}\right)$ is calculated based on the parameter $\mathrm{a}_j\left(\lambda_j^{(r)}\right)$. The iteration continues until convergence is reached for all complex eigenvalues, the calculation of these parameters expressed in Eq. (19). The converged complex eigenvalue is then used to derive the complex eigenvector via the formulation in Eq. (20).

$$\begin{gathered}
\lambda_j^{(r+1)} = -\frac{\eta_j\left(\lambda_j^{(r)}\right)}{2} \pm i\sqrt{\omega_j^2 - \left(\frac{\eta_j\left(\lambda_j^{(r)}\right)}{2}\right)^2}, \\
\mathrm{a}_j\left(\lambda_j^{(r)}\right) = \frac{\lambda_j^{(r)} \mathrm{C}'_{kj}}{\omega_k^2 + \lambda_j^{(r)\,2} + \lambda_j^{(r)} \mathrm{C}'_{kk}}, \forall k \neq j, \\
\eta_j\left(\lambda_j^{(r)}\right) = \mathrm{C}'_{jj} + \mathrm{g}_j^T \mathrm{a}_j\left(\lambda_j^{(r)}\right), \\
\mathrm{g}_j = \left[\mathrm{C}'_{1,j} \quad \mathrm{C}'_{2,j} \quad \cdots \quad j\text{-th terms deleted} \quad \cdots \quad \mathrm{C}'_{N-1,j} \quad \mathrm{C}'_{N,j}\right]
\end{gathered} \tag{19}$$

$$\psi_j\left(\lambda_j^{(r+1)}\right) = \mathrm{q}_j + \sum_{\substack{k=1 \\ k \neq j}}^{N} \mathrm{a}_j\left(\lambda_j^{(r+1)}\right) \mathrm{q}_k, \qquad \forall k \neq j \tag{20}$$

Adhikari's first-order algorithm should terminate computation when the calculated error attains a value equal to or below the specified tolerance error, as expressed below:

$$E_j = \left|\frac{\lambda_j^{(r+1)} - \lambda_j^{(r)}}{\lambda_j^{(r)}}\right| \leq E_{Tol.} \tag{21}$$

Adhikari demonstrated that the first-order iterative algorithm only uses undamped eigenanalysis to compute its solutions with a computation complexity of $\mathrm{O}\left(N^3 + C_l\right)$, where C_l is a parameter related to the number of iterations required to calculate each complex eigensolution using the algorithm. This method is less computationally expensive than the exact state-space method, which has a complexity of $\mathrm{O}\left(2N\right)^3 = \mathrm{O}\left(8N^3\right)$.

https://doi.org/10.37896/pd92.4/9241

ISSN: 0369-8963

2.6 Modal Assurance Criterion and the Modal Frequency Response Functions

The Modal Assurance Criterion (MAC) is a scalar constant. It is used to check the validity of the approximated eigenvector compared to the exact eigenvector by measuring the degree of linearity (consistency) between the two modal vectors. According to Allemang [47], it is possible to calculate the MAC as follows:

$$\mathrm{MAC}(\{\Psi_{App}\},\{\Psi_{exact}\}) = \frac{\left|\{\Psi App\}^{\mathrm{H}}\{\Psi exact\}\right|^2}{\left(\{\Psi App.\}^{\mathrm{H}}\{\Psi App.\}\right)\left(\{\Psi exact\}^{\mathrm{H}}\{\Psi exact\}\right)} \tag{22}$$

$(\bullet)^{\mathrm{H}}$ denotes the Hermitian conjugate transpose.

The modal assurance criterion range is $0 \le \mathrm{MAC} \le 1$. Thus, when the MAC value is close to or equal to one, the approximated complex vector is consistent with the exact complex eigenvector. For more information regarding the modal assurance criterion, refer to [48, 49].

The frequency response functions (FRF) of the dynamic system can be computed using the non-classical complex eigensolutions as follows:

$$\mathrm{H}(i\omega) = \sum_{j=1}^{N}\left[\frac{\mu_j \psi_j \psi_j^T}{i\omega-\lambda_j} + \frac{\mu_j^* \psi_j^* \psi_j^{\mathrm{H}}}{i\omega-\lambda_j^*}\right], \qquad \mu_j = \frac{1}{\psi_j^T\left[2\lambda_j \mathrm{M}+\mathrm{C}\right]\psi_j} \tag{23}$$

The discussion of modal transfer functions is covered in greater detail in reference [50].

https://doi.org/10.37896/pd92.4/9241

ISSN: 0369-8963

3 Numerical study

The study identifies non-classical damping systems by employing diagonal dominance indices. It investigates the effectiveness of the lightly non-classical damping method and Adhikari first-order algorithm in obtaining complex eigensolutions and compares them to the exact state space method. The investigation utilizes a four-degrees-of-freedom structure equipped with three variants of emplacement of viscous dampers in order to analyze three cases of non-classical representations. Variant (a) shows a non-symmetric emplacement of one highly damped viscous damper between the second and third DOFs, variant (b) shows the emplacement of one highly viscous damper between the third and fourth DOFs in a non-symmetric manner, and variant (c) shows the emplacement of two moderately viscous damper symmetrically between the first and second DOFs and the third and fourth DOFs, (Fig. 1 illustrates the structural parameters and damper configurations).

The Adhikari iterative algorithm uses tolerance of $E_{Tol.} = 10^{-4}$. This study considers the external viscous dashpot damping. It omits the inherent structural damping (as indicated in the damping matrices in Eq. (24)). The studied dynamical systems are investigated to validate the correctness of the approximation methods compared with the exact solutions. The study explores the dynamical

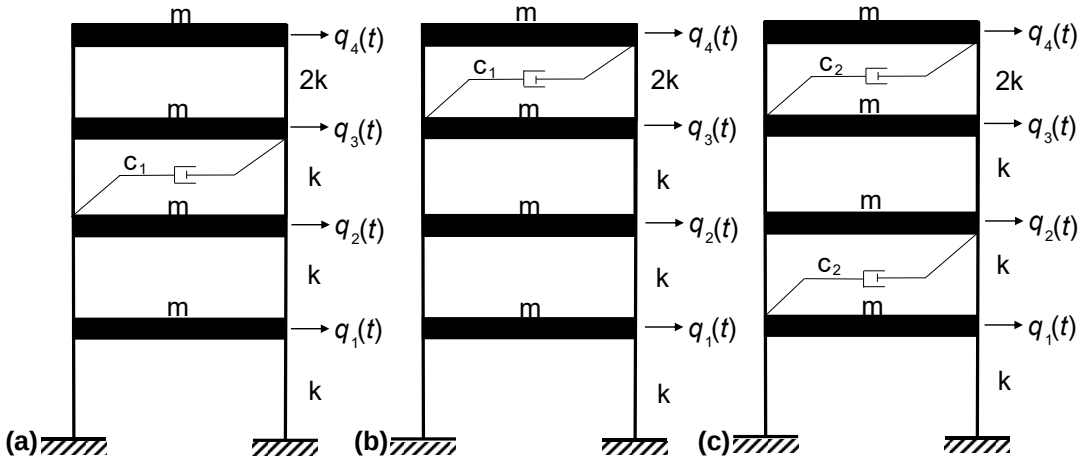

Fig. 1 Three variants of viscous dampers placement in a 4-DOF frame system, $m = 3\times10^3$[kg], $c_1 = 1.35\times10^3$[N.s/m], $c_2 = 6.75\times10^2$[N.s/m] and $k = 2.5\times10^3$[N/m].

characteristics, including diagonality dominance indices, undamped and complex eigenvalues, modal assurance criterion, damping quality factor, damping ratio, damped eigenvalues, and amplitude and phase response outcomes of FRF responses.

$$C_a = c_1\begin{bmatrix}0&0&0&0\\0&1&-1&0\\0&-1&1&0\\0&0&0&0\end{bmatrix},\quad C_b = c_1\begin{bmatrix}0&0&0&0\\0&0&0&0\\0&0&1&-1\\0&0&-1&1\end{bmatrix},\quad C_c = c_2\begin{bmatrix}1&-1&0&0\\-1&1&0&0\\0&0&1&-1\\0&0&-1&1\end{bmatrix} \tag{24}$$

https://doi.org/10.37896/pd92.4/9241

ISSN: 0369-8963

The mass, stiffness, and undamped eigenvectors matrices are represented as:

$$\mathrm{M} = m\begin{bmatrix} 1 & 0 & 0 & 0 \\ 0 & 1 & 0 & 0 \\ 0 & 0 & 1 & 0 \\ 0 & 0 & 0 & 1 \end{bmatrix},\quad \mathrm{K} = k\begin{bmatrix} 2 & -1 & 0 & 0 \\ -1 & 2 & -1 & 0 \\ 0 & -1 & 2 & -1 \\ 0 & 0 & -1 & 2 \end{bmatrix},$$
$$\mathrm{Q} = \begin{bmatrix} 0.2146 & -0.3473 & -0.3473 & -0.2146 \\ 0.3473 & -0.2146 & 0.2146 & 0.3473 \\ 0.3473 & 0.2146 & 0.2146 & -0.3473 \\ 0.2146 & 0.3473 & -0.3473 & 0.2146 \end{bmatrix} \tag{25}$$

The modal damping matrix can be computed from the undamped eigensolutions through Eq. (11). For the three considered variants, the resulting modal damping matrices are represented as follows:

$$\mathrm{C}'_a = \begin{bmatrix} 0 & 0 & 0 & 0 \\ 0 & 0.2488 & 0 & -0.4025 \\ 0 & 0 & 0 & 0 \\ 0 & -0.4025 & 0 & 0.6512 \end{bmatrix}, \mathrm{C}'_b = \begin{bmatrix} 0.0238 & 0.0238 & 0.1006 & -0.1006 \\ -0.0238 & 0.0238 & -0.1006 & 0.1006 \\ 0.1006 & -0.1006 & 0.4262 & -0.4262 \\ -0.1006 & 0.1006 & -0.4262 & 0.4262 \end{bmatrix},$$
$$\mathrm{C}'_c = \begin{bmatrix} 0.0238 & 0 & 0.1006 & 0 \\ 0 & 0.0238 & 0 & 0.1006 \\ 0.1006 & 0 & 0.4262 & 0 \\ 0 & 0.1006 & 0 & 0.4262 \end{bmatrix} \tag{26}$$

The diagonal dominance of the analyzed systems is assessed using $\rho_1(\mathrm{C}')$ and $\rho_2(\mathrm{C}')$. However, Eq. (26) indicates that the matrix C'_a is non-invertible, making applying the $\rho_1(\mathrm{C}')$ diagonality dominance index challenging; this constitutes a novel limitation for this diagonality dominance index in the study of non-classically damped systems, which has not been addressed in previous studies to the author's best knowledge. The outcomes of applying both diagonal dominance indices are shown in Table 1.

Table 1 Diagonality dominance indices results of the modal damping matrices for the three studied variants.

Variant	Diagonality dominance indices	
	ρ [-]	[-]
a	-	1.1180
b	3.0000	0.5279
c	1.0000	2.2361

https://doi.org/10.37896/pd92.4/9241

ISSN: 0369-8963

The results from Table 1 indicate that variant (a) exhibits a near-to-diagonal dominance in the modal damping matrix, while variant (b) demonstrates a strongly non-diagonal dominance due to the high damping and non-linearity caused by the added damper's location. In contrast, variant (c) displays a diagonal dominance modal damping matrix. Notably, the $\rho_1(\mathrm{C}')$ diagonality index was unable to identify the diagonality dominance due to the singularity of the matrix C_a'.

Table 2 A comparison between the eigenvalues of the three studied variants.

Mode	Eigenvalues					
	Undamped	Exact	Lightly non-classical		Adhikari first-order	
j	[rad/s]	[rad/s]	[rad/s]	[%]	[rad/s]	[%]
Variant (a)						
1	0.5642	-0.0000+0.5642i	-0.0000+0.5642i	0.000	-0.0000+0.5642i	0.000
2	1.0731	-0.1220+1.1193i	-0.1244+1.0659i	4.749	-0.1220+1.1193i	0.000
3	1.4771	-0.0000+1.4771i	-0.0000+1.4771i	0.000	-0.0000+1.4771i	0.000
4	1.7364	-0.3280+1.6221i	-0.3256+1.7056i	4.046	-0.3280+1.6221i	0.000
Variant (b)						
1	0.5642	-0.0114+0.5668i	-0.0119+0.5640i	0.497	-0.0117+0.5669i	0.063
2	1.0731	-0.0083+1.0787i	-0.0119+1.0731i	0.621	-0.0093+1.0801i	0.162
3	1.4771	-0.3873+1.5220i	-0.2131+1.4616i	11.737	-0.3804+1.5354i	0.960
4	1.7364	-0.0431+1.6163i	-0.2131+1.7233i	12.426	-0.0403+1.6090i	0.478
Variant (c)						
1	0.5642	-0.0118+0.5656i	-0.0119+0.5641i	0.271	-0.0118+0.5656i	0.000
2	1.0731	-0.0113+1.0759i	-0.0119+1.0731i	0.266	-0.0113+1.0759i	0.000
3	1.4771	-0.2132+1.4576i	-0.2131+1.4616i	0.275	-0.2132+1.4576i	0.000
4	1.7364	-0.2137+1.7186i	-0.2131+1.7233i	0.261	-0.2137+1.7186i	0.000

In Table 2, the complex eigenvalues of the three variants are displayed and calculated using the state-space approach as the exact method, the lightly non-classical damping method, and the Adhikari first-order algorithm. The results reveal that the first and third modes of variant (a) have a zero-decay part (real part), implying that they are not influenced by the damping applied to the system. This observation can be attributed to the damper location and its low level of damping. However, variants (b) and (c) do not exhibit similar behaviour, suggesting that the damping effect in these variants is different from variant (a). Further, in Table 2 variant (a), the lightly non-classical method had a maximum error of 4.749%, considered highly acceptable, while the Adhikari first-order algorithm produced exact results with 0% error. In variant (b), the lightly non-classical method had a maximum error of 12.426%, which was unacceptable. The Adhikari first-order algorithm produced outstanding results with a maximum error of only 0.960%. In variant (c), the lightly non-classical method had a highly acceptable result with a maximum error of 0.275%, and the Adhikari first-order algorithm produced exact results with a 0% error. Eq. (27) can be used to calculate the absolute error between the approximated and the exact complex eigenvalues to evaluate the accuracy of the estimated complex eigenvalues.

$$\mathrm{E}_{\lambda,j}(\%) = \frac{\left|\lambda_{Exact,j} - \lambda_{App.,j}\right|}{\left|\lambda_{Exact,j}\right|} \times 100\% \tag{27}$$

https://doi.org/10.37896/pd92.4/9241

ISSN: 0369-8963

The results of the complex conjugated eigenvalues are visually presented in Fig 2 on a complex plane to provide a clear interpretation.

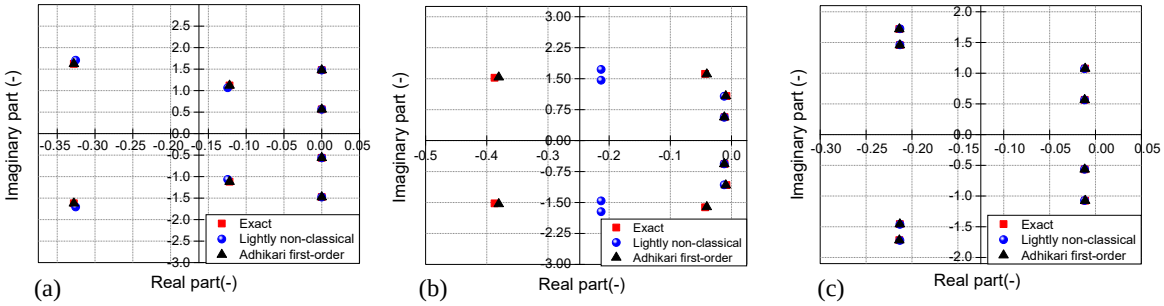

Fig. 2 Comparison in the conjugate complex eigenvalues using the complex plane.

In Table 3, the MAC formulation measures the linearity (consistency) between approximated and exact modal vectors, which enables us to verify the correctness of the estimated complex eigenvectors. Variant (a) displays an unaccepted error with a maximum of 14.80% for the undamped modal vectors. Conversely, the lightly non-classical damping method and Adhikari first-order algorithm show all decoupled eigenvectors with 0% error for all modes. Variant (b) undamped method findings show an unacceptable error with a maximum of 47.60%. The lightly non-classical method yields unacceptably errors of 17.30%, while the Adhikari first-order algorithm yields highly accurate results with a maximum error of 0.90%. Variant (c) undamped method yields highly acceptable results with a maximum error of 0.80%. The lightly non-classical damping method and Adhikari first-order algorithm show all decoupled eigenvectors with 0% error for all modes. The MAC values can be computed using Eq. (22).

Table 3 A comparison between the modal assurance criterion values of the studied three variants.

Mode	Modal assurance criterion					
	Undamped		Lightly non-classical		Adhikari first-order	
j	MAC [-]	ε_{MAC} [%]	MAC [-]	ε_{MAC} [%]	MAC [-]	ε_{MAC} [%]
Variant (a)						
1	1.000	0.000	1.000	0.000	1.000	0.000
2	0.938	6.200	1.000	0.000	1.000	0.000
3	1.000	0.000	1.000	0.000	1.000	0.000
4	0.852	14.800	1.000	0.000	1.000	0.000
Variant (b)						
1	0.998	0.200	1.000	0.000	1.000	0.000
2	0.989	1.100	1.000	0.000	0.999	0.100
3	0.586	41.400	0.827	17.300	0.993	0.700
4	0.524	47.600	0.844	15.600	0.991	0.900
Variant (c)						
1	1.000	0.000	1.000	0.000	1.000	0.000
2	0.997	0.300	1.000	0.000	1.000	0.000
3	0.994	0.600	1.000	0.000	1.000	0.000
4	0.992	0.800	1.000	0.000	1.000	0.000

https://doi.org/10.37896/pd92.4/9241

ISSN: 0369-8963

The error in the modal assurance criterion $E_{MAC,j}$ can be calculated as follows:

$$E_{MAC,j}(\%) = \left|1 - MAC_j\right| \times 100\% \tag{28}$$

The damping quality factor is approximated by Eq. (29) and is used to quantify the degree of modal damping for each mode of the system, which can be used to validate the accuracy of the computed complex eigenvalues.

$$\mathcal{Q}_j = -\frac{\mathrm{Im}}{2\,\mathrm{Re}(\lambda_j)} \tag{29}$$

A lower value of $\mathcal{Q}_j$ results in a larger modal damping level. $\mathcal{Q}_j$ can be conceived as a relation between the real and imaginary parts of the complex mode. Modes with $\mathcal{Q}_j \leq 10$ are classified as highly damped modes, while modes with $\mathcal{Q}_j = \infty$ are classified as undamped modes, according to Lázaro [51].

Table 4 A comparison of the damping quality factor.

Mode	Damping quality factor				
	Exact	Lightly non-classical		Adhikari first-order	
j	$\mathcal{Q}$ [-]	$\mathcal{Q}$ [-]	$\varepsilon_{\mathcal{Q}}$ [%]	$\mathcal{Q}$ [-]	$\varepsilon_{\mathcal{Q}}$ [%]
Variant (a)					
1	∞	∞	0.000	∞	0.000
2	4.587	4.585	6.576	4.586	0.008
3	∞	∞	0.000	∞	0.000
4	2.473	2.619	5.907	2.473	0.000
Variant (b)					
1	24.924	23.743	4.738	24.195	2.927
2	65.027	45.175	30.529	57.780	11.144
3	1.965	3.429	74.506	2.018	2.703
4	18.768	4.043	78.459	19.963	6.368
Variant (c)					
1	24.060	23.746	1.306	24.060	0.000
2	47.680	45.175	5.256	47.681	0.001
3	3.418	3.429	0.332	3.418	0.000
4	4.021	4.043	0.551	4.021	0.000

In Table 4, the approximated quality factor for the three variants can be observed. Variant (a) displays highly accepted results with a maximum error of 6.576% for the lightly non-classical damping method. In comparison, the Adhikari first-order algorithm approximated the exact results with 0% error for all modes. In variant (b), the lightly non-classical damping method failed to accurately capture the exact results, as indicated by a high maximum error of 78.4585%. In contrast, the Adhikari first-order algorithm was highly effective in providing excellent approximations, with a significantly lower maximum error of only 11.145%. In variant (c), the lightly non-classical damping method and the Adhikari first-order algorithm accurately approximated the quality factors. For both methods, the maximum error was less than one, indicating high precision in the estimated values. The following expression can be used to determine the absolute error of quality factors results using approximated complex eigenvalues:

https://doi.org/10.37896/pd92.4/9241

ISSN: 0369-8963

$$E_{\mathcal{Q},j}\left(\%\right)=\frac{\left|\mathcal{Q}_{j,Exact}-\mathcal{Q}_{j,App.}\right|}{\left|\mathcal{Q}_{j,Exact}\right|}\times 100\% \tag{30}$$

The modal damping ratio ζ_j is calculated as follows [52] :

$$\zeta_j=-\frac{\mathrm{Re}\left(\lambda_j\right)}{\mathrm{Im}\left(\lambda_j\right)} \tag{31}$$

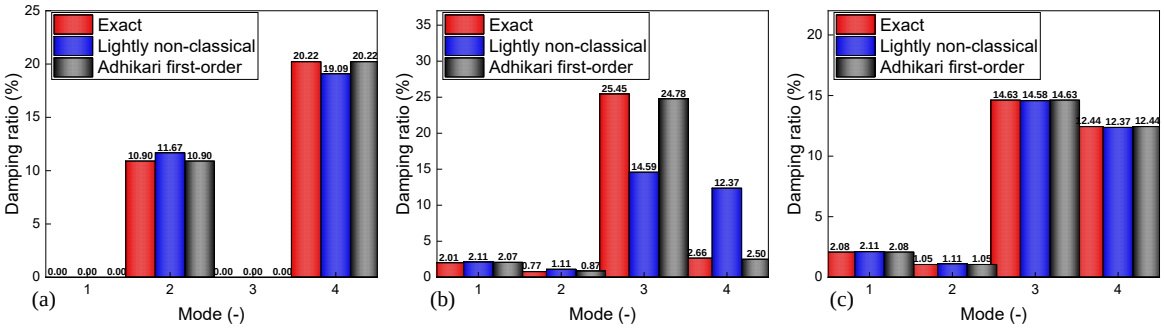

Fig. 3 A comparison of the modal damping ratios.

Figure 3 displays the damping ratios for the three variants that were analyzed. It should be noted that the error in estimating the damping ratio is equivalent to the error in estimating the quality factor. This error is due to the linear relationship between the formulation for the damping ratio and the quality factor.

The damped eigenvalues can be computed from the complex eigenvalues using the following formulation according to Chen et al. [52]:

$$\omega_{d,j}=\sqrt{\left(\mathrm{Re}\left(\lambda_j\right)\right)^2+\left(\mathrm{Im}\left(\lambda_j\right)\right)^2}\equiv\omega_j\sqrt{\left|\zeta_j^2-1\right|} \tag{32}$$

Table 5 A comparison of the damped eigenvalues.

Mode	Damped eigenvalues				
	Exact	Lightly non-classical		Adhikari first-order	
j	ω_d [rad/s]	ω_d [rad/s]	ε_{ω_d} [%]	ω_d [rad/s]	ε_{ω_d} [%]
Variant (a)					
1	0.5642	0.5642	0.000	0.5642	0.000
2	1.0667	1.0658	0.088	1.0667	0.000
3	1.4771	1.4771	0.000	1.4771	0.000
4	1.7005	1.7044	0.231	1.7005	0.000
Variant (b)					
1	0.5641	0.5641	0.002	0.5641	0.001
2	1.0731	1.0731	0.003	1.0731	0.001
3	1.4284	1.4613	2.298	1.4310	0.177
4	1.7358	1.7231	0.732	1.7358	0.004
Variant (c)					
1	0.5641	0.5641	0.001	0.5641	0.000
2	1.0731	1.0731	0.001	1.0731	0.000
3	1.4612	1.4613	0.007	1.4612	0.000
4	1.7229	1.7231	0.009	1.7229	0.000

$$\mathcal{E}_{\omega_{d,j}}\left(\%\right)=\frac{\left|\omega_{d,j,Exact}-\omega_{d,j,App.}\right|}{\left|\omega_{d,j,Exact}\right|}\times 100\% \tag{33}$$

https://doi.org/10.37896/pd92.4/9241

ISSN: 0369-8963

In Table 5, the approximate errors for damped eigenvalues in the three variants are: in variants (a) and (c), the highest error for both the lightly non-classical damping method and the Adhikari first-order algorithm is less than one. Variant (b) estimates outcomes with a maximum error of 2.298% for the lightly non-classical damping method, while Adhikari's first-order algorithm provides excellent approximations with a maximum error of 0.1774 %. The number of iterations required to calculate the eigensolutions using the Adhikari first-order algorithm is presented in Figure 4.

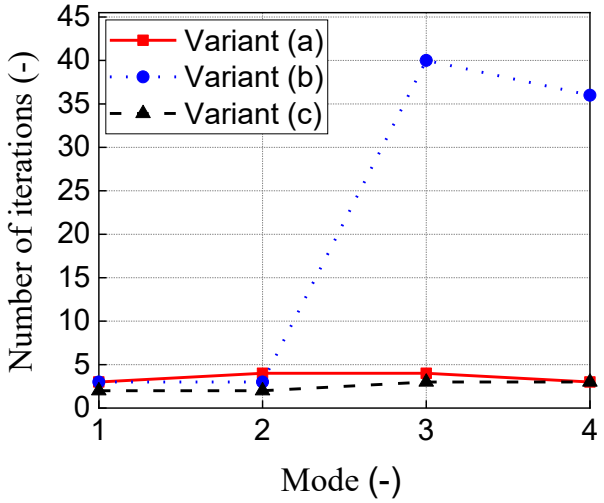

Fig. 4 Index representing the total iterations of the Adhikari first-order algorithm used to find the complex eigensolutions.

Figure 4 shows that the diagonally dominant modes in variants (a) and (c) require less number of iterations for convergence due to their low level of damping non-classicality. On the other hand, in variant (b), the third and fourth modes exhibit a slower convergence rate due to their high coupling, while the other modes of this variant converge faster.

The frequency response functions (FRF) are used in structural dynamics to evaluate dynamic behavior under varying excitation frequencies. The FRFs of the investigated dynamical systems were computed using the exact and approximated complex eigensolutions in Eq. (23). The FRFs were represented by a 4×4 symmetric frequency-dependent matrix $\mathrm{H}(i\omega)$ with distinct complex frequency response functions. The excitation bandwidth covered all undamped natural frequencies. The driving-point FRF $\mathrm{H}(i\omega)_{2,2}$ and cross-FRF $\mathrm{H}(i\omega)_{1,4}$ for each investigated variant were graphically presented in Figs. (5-7). Each figure displayed the amplitude of the FRF (top), the phase response of the FRF (middle), and the difference in approximated and exact FRF amplitude (bottom), with the driving-point FRF on the left and the cross-FRF on the right. The discrepancy between the approximate and actual FRF amplitudes is calculated as follows:

$$\Delta Amplitude = Amplitude\left(Exact\right) - Amplitude\left(App.\right) \tag{34}$$

https://doi.org/10.37896/pd92.4/9241

ISSN: 0369-8963

In the FRF amplitude section, it is crucial to note the direct correlation between the modal damping and resonance peak occurrence. When the modal damping is low, the FRF amplitudes exhibit high and narrow resonant peaks. In contrast, the resonance peak is wider when the modal damping is high.

Figure 5 illustrates that in variant (a), the first and second modes exhibit low modal damping, resulting in only two resonance peaks in the driving-point-FRF and cross-FRF results. The FRF amplitudes and phase responses obtained using the lightly non-classical damping method and the Adhikari first-order algorithm are nearly identical to the exact results, with no notable errors.

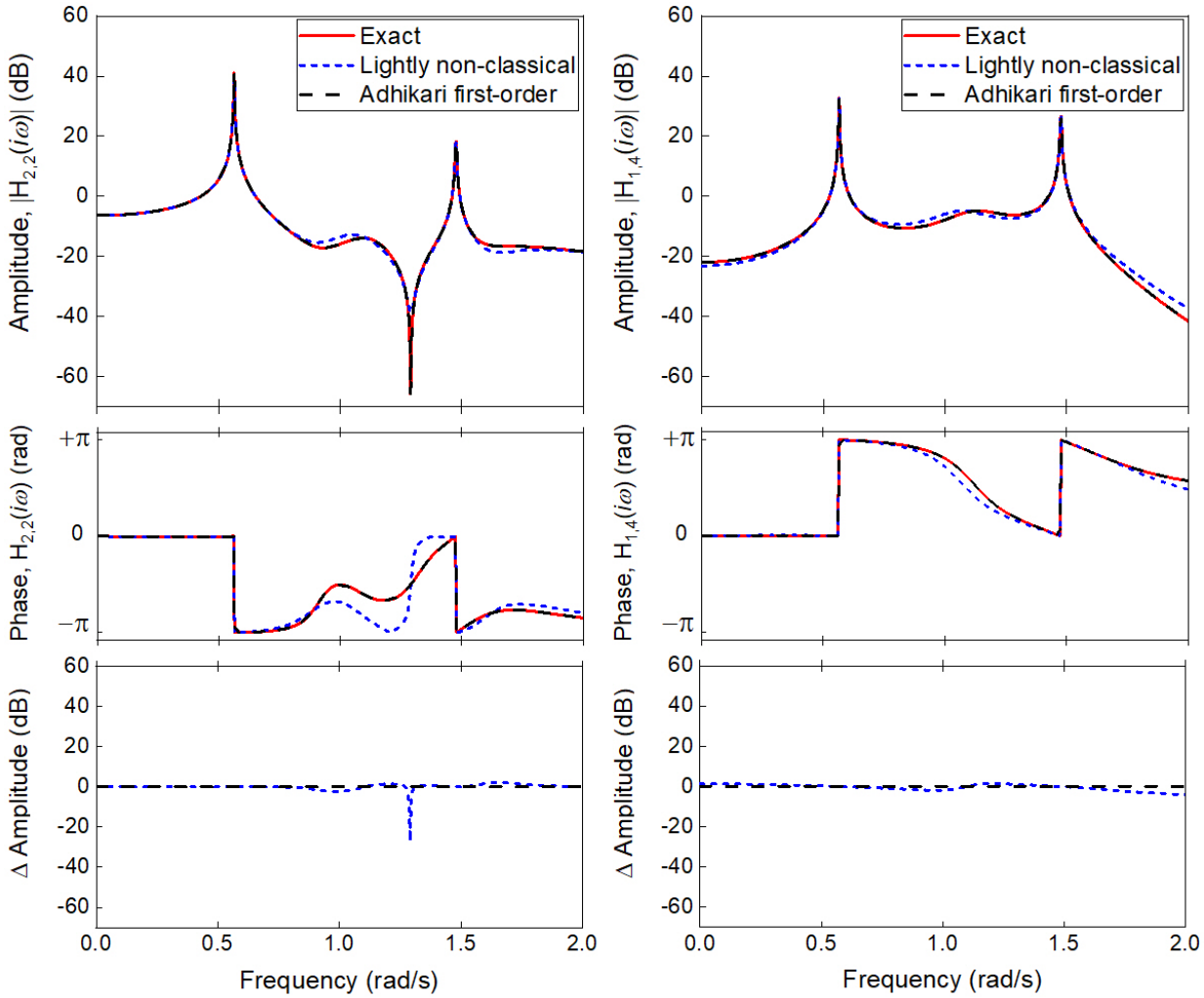

Fig. 5 A comparison in the FRF responses of the variant (a): for the $\mathrm{H}(i\omega)_{2,2}$ in left, for the $\mathrm{H}(i\omega)_{1,4}$ in the right.

https://doi.org/10.37896/pd92.4/9241

ISSN: 0369-8963

In Figure 6, due to the low modal damping of the first, second, and fourth modes in variant (b), three resonance peaks are visible in the results of the driving-point-FRF and the cross-FRF. The lightly non-classical damping method failed to approximate the exact results of the FRF responses, which can be observed by seeing that the third peak is not visible. This phenomenon, called fictional damping, happens when the modal coupling is so high (For further information about fictional damping due to the classical damping hypothesis, see [35]). On the other hand, Adhikari's first-order algorithm approximates the exact FRF amplitude and phase response results.

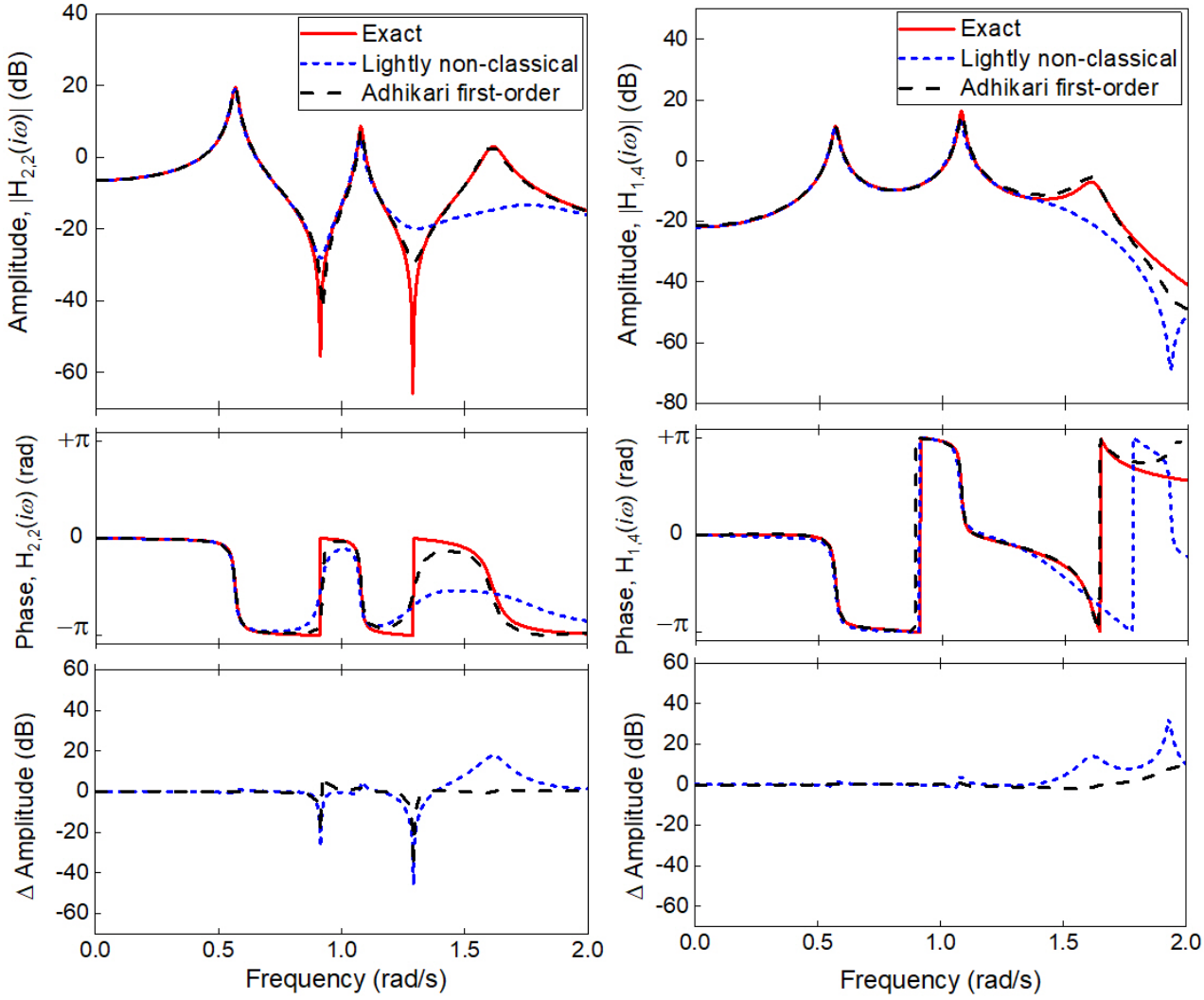

Fig. 6 A comparison in the FRF responses of the variant (b): for the $H(i\omega)_{2,2}$ in left, for the $H(i\omega)_{1,4}$ in the right.

https://doi.org/10.37896/pd92.4/9241

ISSN: 0369-8963

As shown in Fig. 7, due to the low modal damping of the first and second modes in variant (c), only two resonance peaks are visible in the results of the driving-point-FRF and the cross-FRF. Compared to the exact results, the FRF amplitude and phase response calculated using the lightly non-classical damping method and the Adhikari first-order algorithm are very close, without any noteworthy errors.

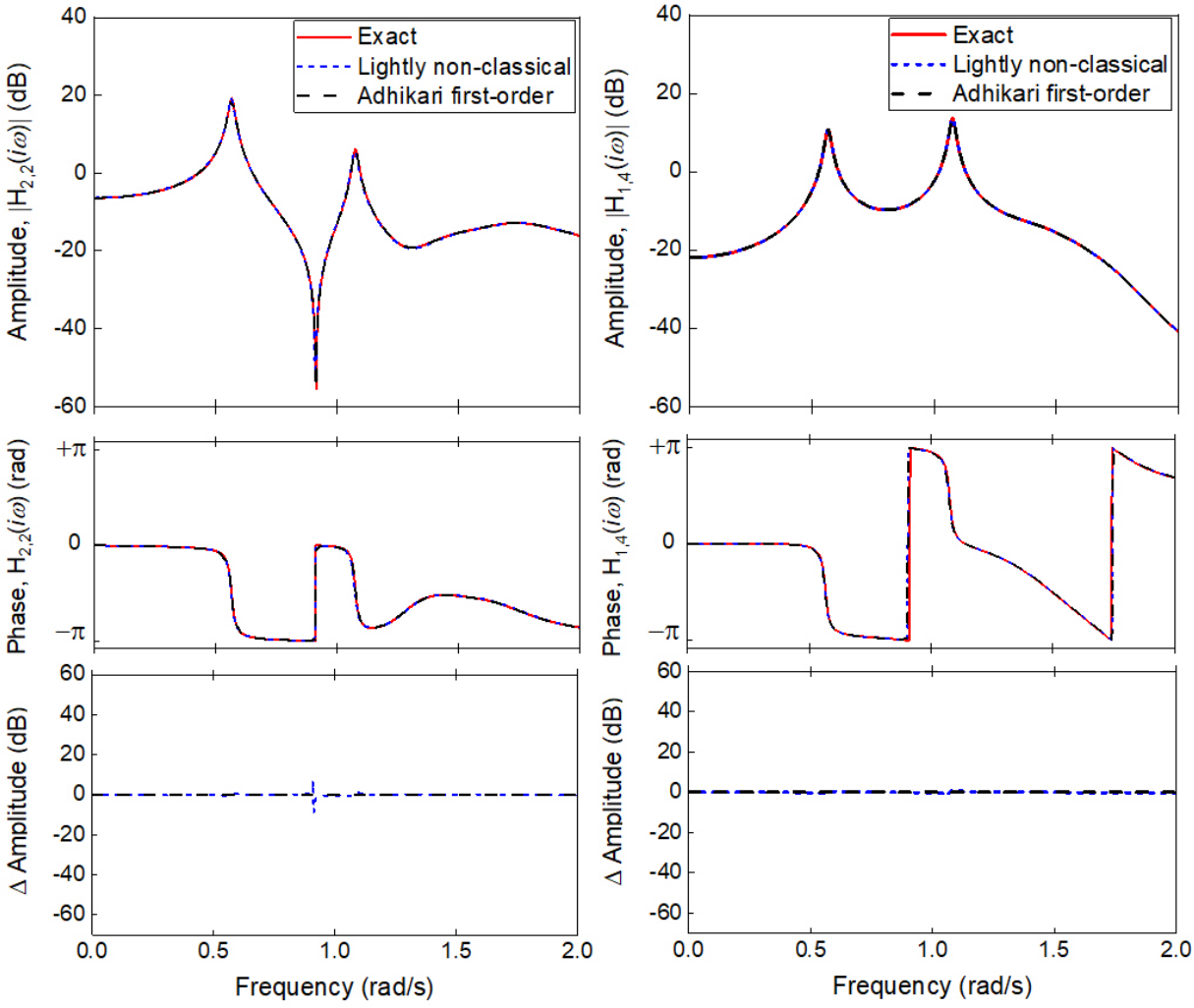

Fig. 7 A comparison in the FRF responses of the variant (c): for the $\mathrm{H}(i\omega)_{2,2}$ in left, for the $\mathrm{H}(i\omega)_{1,4}$ in the right.

https://doi.org/10.37896/pd92.4/9241

ISSN: 0369-8963

In Fig. 8-a, by comparing the diagonal dominance index ρ_2 from Table 1 and the minimum MAC values from Table 3, the data shows a direct correlation between diagonal dominance and modal decoupling of the eigenvectors. The Adhikari first-order algorithm provides highly decoupled eigenvectors across the range of ρ_2 values with MAC values close to one. The undamped eigenvectors show a highly modal coupling when ρ_2 is less than one. In contrast, the lightly non-classical damping method fully decoupled the eigenvectors correctly using the formulation in Eq. (17) only when the ρ_2 is more significant than one.

Fig. 8-b shows a direct correlation between the diagonal dominance index ρ_2 and the error of the computed eigenvalues (the relative absolute error in the complex eigenvalues) from Table 2. The Adhikari first-order algorithm can accurately predict complex eigenvalues over a range of ρ_2 values, with typical errors falling around 1%. On the other hand, the lightly non-classical damping method has a significant error when the ρ_2 is below one and a tolerable error when the system is uncoupled (i.e., ρ_2 is more than or equal to one).

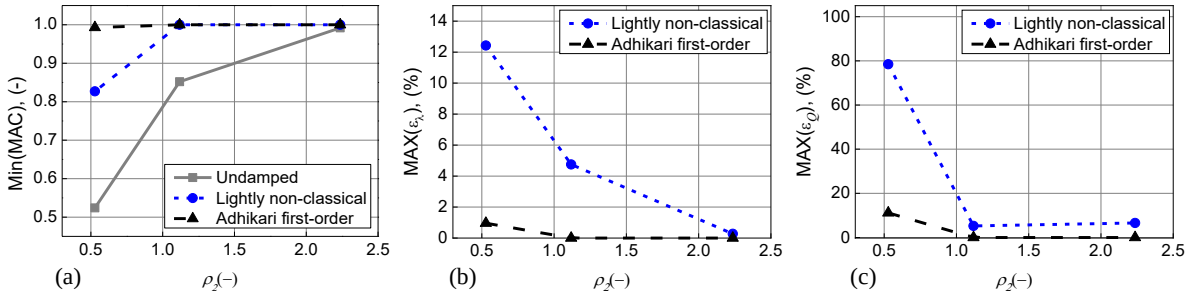

Fig. 8 The diagonal dominance index a) in relation to the minimum MAC values of the estimated eigenvectors, b) in relation to the maximum error in complex values, and c) in relation to the maximum error in quality factors.

As shown in Fig. 8-c, the quality factor uses to verify that the real and imaginary components of the complex eigensolutions are in equilibrium. A comparison between the diagonal dominance index and the maximum error in the computed damping quality factor from Table 4; shows that for ρ_2 smaller than one, the Adhikari first-order algorithm results are considered acceptable, with a maximum inaccuracy of about 11%. However, it produces extremely precise outcomes when ρ_2 is greater than or equal to one. By contrast, when the ρ_2 is less than one, the lightly non-classical damping method has a substantial error due to the modal coupling, with an error of more than 78%, a reasonable allowance for error after the system is decoupled (i.e., ρ_2 is more than or equal to one).

https://doi.org/10.37896/pd92.4/9241

ISSN: 0369-8963

To summarize their findings, the authors propose a new subspace algorithm to approximate non-classical complex eigensolutions. The algorithm first determines the degree of diagonality dominance and selects the appropriate method, either the lightly non-classical damping method or the Adhikari first-order algorithm [26]. For the lightly non-classical damping method, the algorithm further improves the decoupling of undamped modes using a simple formula found in [30]. Compared to the state space method, which computes all non-classical complex eigensolutions simultaneously in a double-size eigenvalue problem, the proposed algorithm adopts a more systematic approach. It uses a sub-iterative frame to solve the quadratic eigenvalue problem in its original form for a selected range of complex eigensolutions. This approach enables the rapid finding of solutions for specific ranges of complex eigensolutions. The function formulation of the proposed algorithm is presented in Fig. 9.

Function $[\lambda, \boldsymbol{\psi}] = decoupling(\Omega, Q, C', \rho_2, N, N_c, \varepsilon_{Tol})$

for $j = 1 : N_c$ do

if $\rho_2(\mathbf{C}') < 1$ do

$r = 0, \varepsilon = 10;$

$\mathbf{g}_j = \left[\mathbf{C}'_{1,j} \quad \mathbf{C}'_{2,j} \quad \cdots \quad j\text{th terms deleted} \quad \cdots \quad \mathbf{C}'_{N-1,j} \quad \mathbf{C}'_{N,j} \right]$

$$\lambda_j^{(r)} = -\frac{\mathbf{C}_{jj}}{2} \pm i\sqrt{\omega_j^2 - \left(\frac{\mathbf{C}_{jj}}{2}\right)^2},$$

while $\varepsilon > \varepsilon_{Tol}$ do

$$\mathbf{a}_j\left(\lambda_j^{(r)}\right) = \frac{\lambda_j^{(r)} \mathbf{C}'_{kj}}{\omega_k^2 + \lambda_j^{(r)2} + \lambda_j^{(r)} \mathbf{C}'_{kk}}$$

$$\boldsymbol{\eta}_j\left(\lambda_j^{(r)}\right) = \mathbf{C}'_{jj} + \mathbf{g}_j^T \mathbf{a}_j\left(\lambda_j^{(r)}\right),$$

$$\lambda_j^{(r+1)} = -\frac{\boldsymbol{\eta}_j\left(\lambda_j^{(r)}\right)}{2} \pm i\sqrt{\omega_j^2 - \left(\frac{\boldsymbol{\eta}_j\left(\lambda_j^{(r)}\right)}{2}\right)^2},$$

$$\varepsilon = \left| \frac{\lambda_j^{(r+1)} - \lambda_j^{(r)}}{\lambda_j^{(r)}} \right|$$

$r = r + 1;$

end while

$$\boldsymbol{\psi}_j\left(\lambda_j^{(r)}\right) = \mathbf{q}_j + \sum_{\substack{k=1 \\ k \neq j}}^{N} \mathbf{a}_j\left(\lambda_j^{(r)}\right) \mathbf{q}_k,$$

end if

elseif

$$\lambda_j = -\frac{\mathbf{C}_{jj}}{2} \pm i\sqrt{\omega_j^2 - \left(\frac{\mathbf{C}_{jj}}{2}\right)^2},$$

$$\boldsymbol{\psi}_j = \mathbf{q}_j + \sum_{\substack{k=1 \\ k \neq j}}^{N} \frac{\lambda_j \mathbf{C}'_{kj}}{\omega_k^2 + \lambda_j^2 + \lambda_j \mathbf{C}'_{kk}} \mathbf{q}_k$$

end elseif

end for

end Function

Fig. 9 The newly formulated subspace algorithm to decouple the non-classically linear damped systems.

https://doi.org/10.37896/pd92.4/9241

ISSN: 0369-8963

Parameters N, N_c, and $E_{Tol.}$ stand for the length of the eigenvalue problem (which may be derived using Eq. (35)), the corresponding number of modes to be calculated, and the error tolerance of the Adhikari first order algorithm, respectively.

$$N = \text{length}(\text{M}) \tag{35}$$

This method requires the lightly non-classical complex eigenvalues from Eq. (16), the modal damping matrix from Eq. (11), and the undamped eigenvectors from Eq. (9) as initial values.

4 Conclusion

This research paper investigates the non-classicality of damping and the modal decoupling of non-classical linear damped systems. Two overall diagonality dominance indices based on the undamped eigensolutions were used to identify the non-classicality of the damping. The lightly non-classical damping method and Adhikari's first-order algorithm were compared in a modal parameters investigation of a 4-DOF frame system with three variants of external damping characteristics. The results show that the lightly non-classical damping method is effective for dominant diagonal cases, while the Adhikari first-order algorithm is necessary for non-diagonal dominant cases. The funding has clearly shown that modal coupling can significantly impact the estimation of the damping loss factor, leading to an incorrect estimation. This coupling can also affect the accuracy of capturing the FRF responses.

The following ideas can be outlined.

- When $(\rho_2 \approx 1)$, as in variant (a) of this study, the damping system is lightly non-classical and diagonal dominant. In such cases, the lightly non-classical damping method can provide robustly approximated complex eigenvalues and fully decoupled complex eigenvectors, as proven by tracking the modal assurance criterion results when using a correction formulation.
- When $(\rho_2 \prec 1)$, as in variant (b) of this study, the damping system is highly non-classical and exhibits modal coupling. In such cases, the lightly non-classical damping method may not produce accurate complex eigensolutions. Adhikari's first-order algorithm may be necessary to improve the prediction of complex eigensolutions.
- When $(\rho_2 \succ 1)$, as in variant (c) of this study, the damping system is lightly damped and diagonal dominant. Both investigated methods can robustly predict complex eigensolutions of non-classical systems in such cases.

The study proposes a new subspace algorithm that combines the two methods investigated in the study. This algorithm utilizes diagonality dominance identification and then improves the performance of the lightly non-classical damping method by enhancing the decoupling of eigenvectors. This new algorithm can efficiently approximate non-classical complex eigensolutions and provides a practical approach for computing such solutions. This algorithm can benefit researchers and engineers who analyze and design structures with non-classical damping.

 https://doi.org/10.37896/pd92.4/9241

Acknowledgment

The authors thank the Directorate General for Scientific Research and Technological Development (DGRSDT), Algeria.

References

1. Lord R (1887) The theory of sound (two volumes). reissued 1945, second edition, Dover Publications, New York
2. Caughey T, O'Kelly M E (1965) Classical normal modes in damped linear dynamic systems. ASME Journal of Applied Mechanics **32**:583-588.
3. Ma F, Imam A, Morzfeld M (2008) Extension of Modal Analysis to Decouple All Linear Systems in Oscillatory Free Vibration. in: International Design Engineering Technical Conferences and Computers and Information in Engineering Conference. pp. 557-561.
4. Koruk H, Sanliturk K Y (2013) A novel definition for quantification of mode shape complexity. Journal of Sound and Vibration **332**(14):3390-3403.
5. Nerse C, Wang S (2019) On the formation of complex modes in non-proportionally damped systems. Journal of Sound and Vibration **463**:114978.
6. Imregun M, Ewins D (1995) Complex modes-origins and limits. in: Proceedings of the 13th International Modal Analysis Conference (IMAC). pp. 496-506.
7. Behnamfar F, Alibabaei H (2017) Classical and non-classical time history and spectrum analysis of soil-structure interaction systems. Bulletin of Earthquake Engineering **15**:931-965.
8. Zhang Z, Wei H, Qin X (2017) Experimental study on damping characteristics of soil-structure interaction system based on shaking table test. Soil Dynamics and Earthquake Engineering **98**:183-190.
9. Cruz C, Miranda E (2017) Evaluation of soil-structure interaction effects on the damping ratios of buildings subjected to earthquakes. Soil Dynamics and Earthquake Engineering **100**:183-195.
10. Li L, Hu Y, Wang X (2014) Harmonic response calculation of viscoelastic structures using classical normal modes: An iterative method. Computers & Structures **133**:39-50.
11. Ding Z, Li L, Hu Y (2018) A modified precise integration method for transient dynamic analysis in structural systems with multiple damping models. Mechanical Systems and Signal Processing **98**:613-633.
12. Gao Y, Zhang S, Zhao G, Schmidt R (2022) Numerical modeling for cantilever sandwich smart structures with partially covered constrained viscoelastic layer. Composite Structures **281**:114981.
13. De Domenico D, Falsone G, Ricciardi G (2018) Improved response-spectrum analysis of base-isolated buildings: a substructure-based response spectrum method. Engineering structures **162**:198-212.
14. Nasr A, Mrad C, Nasri R (2023) Explicit Formulas for Optimal Parameters of Friction Dynamic Vibration Absorber Attached to a Damped System Under Various Excitations. Journal of Vibration Engineering & Technologies **11**(1):85-97.
15. Tisseur F, Meerbergen K (2001) The quadratic eigenvalue problem. SIAM review **43**(2):235-286.
16. Walsh T F, Day D M (2007) Quadratic eigenvalue problems(Report No.SAND2007-2072), Sandia National Laboratories (SNL), Albuquerque, United States of America

17. Li L, Hu Y, Wang X (2016) Accurate method for harmonic responses of non-classically damped systems in the middle frequency range. Journal of Vibration and Control **22**(2):426-441.

18. Fischer P (2000) Eigensolution of nonclassically damped structures by complex subspace iteration. Computer methods in applied mechanics and engineering **189**(1):149-166.

19. Holz U B, Golub G H, Law K H (2004) A subspace approximation method for the quadratic eigenvalue problem. SIAM journal on matrix analysis and applications **26**(2):498-521.

20. Łasecka-Plura M, Lewandowski R (2021) The subspace iteration method for nonlinear eigenvalue problems occurring in the dynamics of structures with viscoelastic elements. Computers & Structures **254**:106571.

21. Rajakumar C (1993) Lanczos algorithm for the quadratic eigenvalue problem in engineering applications. Computer methods in applied mechanics and engineering **105**(1):1-22.

22. Cha P D (2005) Approximate eigensolutions for arbitrarily damped nearly proportional systems. Journal of Sound and Vibration **288**(4-5):813-827.

23. Cortés F, Elejabarrieta M J (2006) Computational methods for complex eigenproblems in finite element analysis of structural systems with viscoelastic damping treatments. Computer methods in applied mechanics and engineering **195**(44-47):6448-6462.

24. Özgüven H N (2002) Twenty years of computational methods for harmonic response analysis of non-proportionally damped systems. in: International Modal Analysis Conference IMAC XX. pp. 390-396.

25. Ma F, Morzfeld M, Imam A (2010) The decoupling of damped linear systems in free or forced vibration. Journal of Sound and Vibration **329**(15):3182-3202.

26. Adhikari S (2011) An iterative approach for nonproportionally damped systems. Mechanics Research Communications **38**(3):226-230.

27. Lázaro M (2016) Eigensolutions of non-proportionally damped systems based on continuous damping sensitivity. Journal of Sound and Vibration **363**:532-544.

28. Hračov S, Náprstek J (2017) Approximate complex eigensolution of proportionally damped linear systems supplemented with a passive damper. Procedia engineering **199**:1677-1682.

29. Lázaro M (2018) Eigensolutions of nonviscously damped systems based on the fixed-point iteration. Journal of Sound and Vibration **418**:100-121.

30. Adhikari S (1999) Modal analysis of linear asymmetric nonconservative systems. Journal of Engineering Mechanics **125**(12):1372-1379.

31. Sinha A (2020) Computing eigenvalues, eigenvectors and frequency responses of structures with non-proportional damping. Journal of Sound and Vibration **489**:115681.

32. Morzfeld M, Ma F, Parlett B N (2011) The transformation of second-order linear systems into independent equations. SIAM Journal on Applied Mathematics **71**(4):1026-1043.

33. Denoël V, Degée H (2009) Asymptotic expansion of slightly coupled modal dynamic transfer functions. Journal of Sound and Vibration **328**(1-2):1-8.

34. Morzfeld M, Ma F, Ajavakom N (2008) On the decoupling approximation in damped linear systems. Journal of Vibration and Control **14**(12):1869-1884.

35. Anajafi H, Medina R A, Santini-Bell E (2020) Effects of the improper modeling of viscous damping on the first-mode and higher-mode dominated responses of base-isolated buildings. Earthquake engineering & structural dynamics **49**(1):51-73.

 https://doi.org/10.37896/pd92.4/9241

ISSN: 0369-8963

36. Warburton G, Soni S (1977) Errors in response calculations for non-classically damped structures. Earthquake engineering & structural dynamics **5**(4):365-376.

37. Hasselman T (1976) Modal coupling in lightly damped structures. AIAA Journal **14**(11):1627-1628.

38. Park I, Kim J, Ma F (1992) On modal coupling in non-classically damped linear systems. Mechanics Research Communications **19**(5):407-413.

39. Morzfeld M, Ajavakom N, Ma F (2009) Diagonal dominance of damping and the decoupling approximation in linear vibratory systems. Journal of Sound and Vibration **320**(1-2):406-420.

40. Bajrić A, Høgsberg J (2018) Identification of damping and complex modes in structural vibrations. Journal of Sound and Vibration **431**:367-389.

41. Foss K A (1958) Co-ordinates which uncouple the equations of motion of damped linear dynamic systems. J. Appl. Mech. **25**:361-364.

42. Gawronski W, Sawicki J T (1997) Response errors of non-proportionally lightly damped structures. Journal of Sound and Vibration **200**(4):543-550.

43. Park I, Kim J, Ma F (1994) Characteristics of modal coupling in nonclassically damped systems under harmonic excitation. J. Appl. Mech. **61**(1):77-83.

44. Graham A (1987) Nonnegative Matrices and Applicable Topics in Linear Algebra. Halsted Press, New York

45. Canor T, Blaise N, Denoël V (2012) Efficient uncoupled stochastic analysis with non-proportional damping. Journal of Sound and Vibration **331**(24):5283-5291.

46. Ibrahimbegovic A, Wilson E L (1989) Simple numerical algorithms for the mode superposition analysis of linear structural systems with non-proportional damping. Computers & Structures **33**(2):523-531.

47. Allemang R J (2003) The modal assurance criterion–twenty years of use and abuse. Sound and vibration **37**(8):14-23.

48. Pastor M, Binda M, Harčarik T (2012) Modal assurance criterion. Procedia engineering **48**:543-548.

49. Li L, Hu Y, Wang X (2014) Direct way of computing the variability of modal assurance criteria. Mechanics Research Communications **55**:53-58.

50. Balmès E (1996) Frequency domain identification of structural dynamics using the pole/residue parametrization. in: Proceedings of the International Modal Analysis Conference. pp. 540–546.

51. Lázaro M (2015) Nonviscous modes of nonproportionally damped viscoelastic systems. Journal of Applied Mechanics **82**(12):121011.

52. Chen H, Tan P, Zhou F (2017) An improved response spectrum method for non-classically damped systems. Bulletin of Earthquake Engineering **15**(10):4375-4397.

 https://doi.org/10.37896/pd92.4/9241